Journal of Experimental Nanoscience
Publication details, including instructions for authors and subscription information:
http://www.informaworld.com/smpp/title~content=t716100757

Onion-like carbon synthesis by annealing nanodiamond at lower temperature and vacuum

Q. Zou[a]; M. Z. Wang[a]; Y. G. Li[a]
[a] State Key Laboratory of Metastable Materials Science and Technology, Yanshan University, Qinhuangdao 066004, Hebei, People's Republic of China

Online publication date: 05 November 2010

To cite this Article Zou, Q. , Wang, M. Z. and Li, Y. G.(2010) 'Onion-like carbon synthesis by annealing nanodiamond at lower temperature and vacuum', Journal of Experimental Nanoscience, 5: 5, 375 — 382
To link to this Article: DOI: 10.1080/17458080903583899
URL: http://dx.doi.org/10.1080/17458080903583899

Journal of Experimental Nanoscience
Vol. 5, No. 5, October 2010, 375–382

Taylor & Francis
Taylor & Francis Group

Onion-like carbon synthesis by annealing nanodiamond at lower temperature and vacuum

Q. Zou*, M.Z. Wang and Y.G. Li

State Key Laboratory of Metastable Materials Science and Technology, Yanshan University, Qinhuangdao 066004, Hebei, People's Republic of China

(*Received 19 December 2008; final version received 28 December 2009*)

The onion-like carbon (OLC) was synthesised by annealing the nanodiamond fabricated by detonation for 1 h at the temperature of 1150°C in the low vacuum of 2 Pa. The OLC particles were characterised using a high-resolution transmission electron microscope (HRTEM) for observing its microstructure, an X-ray diffractometer (XRD) for determining its crystal structure and component, and a Raman spectrometer for confirming its content. The results showed that the OLC particles exhibited similar shape to that of the original nanodiamond particles. The average size of the OLC was found to be approximately 5 nm. The transformation mechanism of the OLC from the nanodiamond by annealing at lower temperature and lower vacuum was also discussed.

Keywords: onion-like carbon; nanodiamond; annealing; transformation; characterisation

1. Introduction

Onion-like carbon (OLC) is a member of the fullerene family, which is a three-dimensional structure closed carbon particle consisting of multi-layer concentric carbon sphere. Professor Iijima [1] observed concentric rings with spacing of about 0.34 nm when he studied the carbon film prepared by the method of arc discharge (vacuum, no protective atmosphere) in a high-resolution transmission electron microscope (HRTEM). Moreover, he pointed out that the diameter of the innermost layer small ring was approximately 0.71 nm, which was clearly the OLC fabricated through fragment graphite bending and closure. This was the first OLC observed. However, at that time, his work was not taken seriously because C_{60} had not yet been characterised. OLC attracted much more attentions since Ugarte's discovery [2].

Due to its unique structural and physical properties, OLC has been widely applied in many fields, including nanoball bearings, nanoelectronic-magnetic devices [3,4], gas storage [5,6], biotechnology [7], high-conductors or even superconductors [8], lubricants and rubber intensifiers [9], radioactive tracers and radioactive substances, new materials of

*Corresponding author. Email: 1465314@qq.com

ISSN 1745–8080 print/ISSN 1745–8099 online

DOI: 10.1080/17458080903583899
http://www.informaworld.com

contrast agents [10,11], photovoltaic and fuel cells [12,13], stable reaction clusters in chemistry and special performances catalysts [14].

During the past few years, a number of methods have been reported, such as annealing soot or nanodiamond in vacuum [15], bombarding high-energy electrons onto carbon soot in a HRTEM, implanting carbon ion into copper or silver at high temperatures, radio-frequency (rf) plasma chemical vapour deposition [16] and arc discharge in water [17] for manufacturing OLC. At the present time, the most effective method for fabricating OLC is by annealing nanodiamond particles synthesised by detonation in vacuum at fixed temperatures. However, for the OLC fabrication by annealing nanodiamond synthesised by detonation in vacuum, the reported lowest temperature is from 1100°C to 1200°C [18] and the lowest vacuum is 1.0×10^{-6} Torr [19], respectively. These conditions are very difficult for realising the volume-production of the OLC, which limits its applications. Furthermore, mechanism for the transformation of the nanodiamond into OLC by annealing in vacuum is not clear.

In this work, OLC was synthesised by annealing the nanodiamond synthesised by detonation for 1 h at the temperature of 1150°C in the low vacuum of 2 Pa. The mechanism for the transformation of the nanodiamond into OLC is presented below.

2. Experimental details

The nanodiamond used in this work was obtained from Shenzhen City Diamond Source New Material Development Co., Ltd. (P. R. China). The nanodiamond was fabricated by the method of TNT detonation under the absence of oxygen. The pressure and the temperature were from 2.0 to 3.0 GPa and from 2000 to 3000 K [20], respectively, during the detonation. The purification of the nanodiamond was carried out with a hot mixture of concentrated H_2SO_4 and $HClO_4$ acids in the 1 : 1 ratio in order to remove the amorphous carbon and the graphite after the detonation. The nanodiamond particles had an average size of about 5 nm. However, particle size varied from 2 to 12 nm. The details on the microstructures, the surface states and the physical properties of the nanodiamond have already been published in a previous paper [21].

The annealing experiments for fabricating the OLC were carried out in a vacuum carbon furnace (ZT−25−20 type, Shanghai Chenrong Electric Furnace Co., Ltd., P. R. China). The chamber size of the furnace was φ, 90 × 120 mm. The rated power was 25 kW, the working voltage was from 0 to 27 V. The rated temperature was approximately 2000°C and the cold limited vacuum was $6–7 \times 10^{-3}$ Pa. The nanodiamond powder was put in a graphite tube at first. Then the tube was placed in the furnace chamber. The furnace chamber was vacuumed up to 2 Pa by a mechanical pump and a proliferation pump. However, a cold trap using liquid nitrogen was applied in the vacuum line between the diffusion pump and the furnace chamber, which prevented the oil from being into the furnace vacuum chamber. Then it was heated up to 1150°C and kept for 1 h. The annealing temperature was raised at a rate of 15°C/min. Finally, the annealed samples were cooled to the room temperature in the furnace vacuum chamber.

A HRTEM was used to characterise the microstructures of the nanodiamond and the OLC as-fabricated. An X-ray diffractometer (XRD) was used to determine the crystalline microstructure and the containing elements of the sample annealed. A Raman spectrometer was used to determine the sample species. The HRTEM experiments were carried out

on a JEM-2010 microscope (Japan) at 200 keV with a point resolution of 0.21 nm. In the HRTEM experiments, samples were dispersed in ethanol by ultrasonication and then deposited on copper grids. The XRD experiments were carried out on a D/MAX-2500/PC diffractometer (Japan) using Cu Kα radiation. Raman spectra were obtained using EQUINO × 55-type equipment (Germany).

3. Results and discussion

Figure 1 shows the HRTEM images of the nanodiamond and the OLC as-fabricated. In Figure 1(a), we can see that the outlines of the particles were clear and the particles took on diverse shapes. The nanodiamond particle size was in the range from 2 to 12 nm. However, the average size of the nanodiamond was approximately 5 nm. Lattice fringes corresponding to the (1 1 1) planes of diamond were obviously observed. The interlayer spacing was about 0.206 nm, as shown in Figure 1(a), which agreed with that of the diamond (1 1 1) planes. Figure 1(b) presents the HRTEM image of the OLC annealed from the nanodiamond for 1 h and at the temperature of 1150°C. As seen in Figure 1(b), almost all the nanodiamond particles were transformed into the OLC annealed for 1 h and at the temperature of 1150°C. Moreover, the OLC took on diverse shapes including quasi-spherical, elliptical, polyhedral and deformed onions. The shapes of the OLC were similar to that of the original nanodiamond. The average size of the OLC was approximately 5 nm. The layers of the OLC were varied from several to 12. The spacing between the interlayer was about 0.34 nm.

Figure 2 shows the selected area diffraction (SAD) patterns of the nanodiamond and the OLC as-fabricated. From the SAD pattern of the nanodiamond shown in Figure 2(a), it is clear that the SAD pattern of the nanodiamond had three clear circle, which corresponded to the (1 1 1), (2 2 0) and (3 1 1) crystal plane diffraction of the nanodiamond, respectively, from the internal to the external. This demonstrated that the nanodiamond

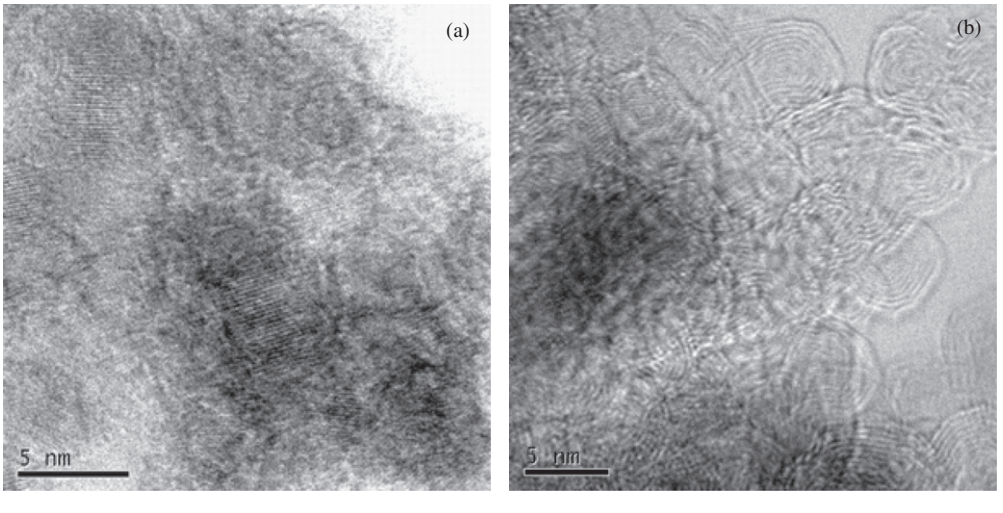

Figure 1. HRTEM images of (a) nanodiamond and (b) OLC.

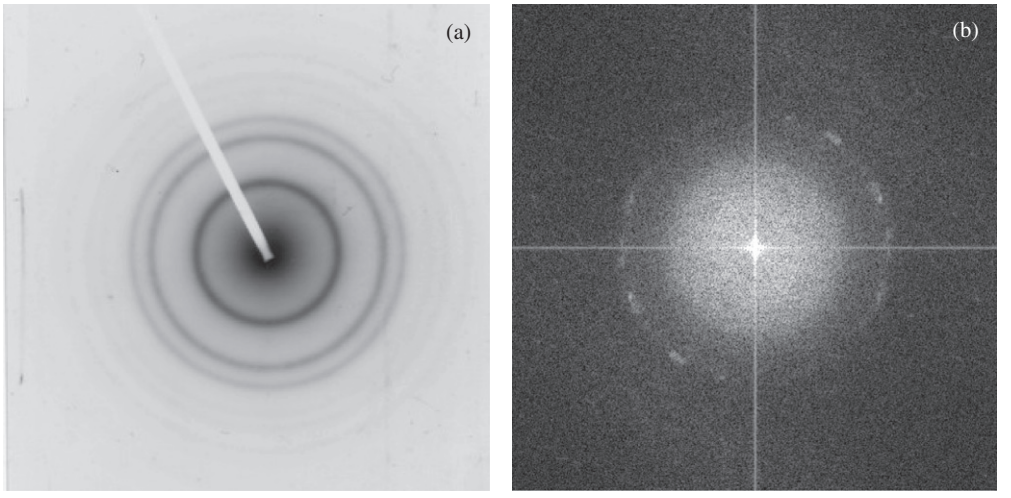

Figure 2. SAD patterns of (a) nanodiamond and (b) OLC.

was cubic diamond. Furthermore, the SAD pattern of the nanodiamond exhibited a wide (1 1 1) line, which was evidently due to both the high dispersion and imperfection of the particles, whose shape was approximately spherical. This was characteristic of detonation-synthesised nanodiamond particles [22,23]. From Figure 2(b), we can see that the OLC crystal structure coexisted with the amorphous carbon structure in the centre of the OLC particle, which was agreed with the result of the OLC HRTEM image shown in Figure 1(b).

Figure 3 shows the XRD patterns of the nanodiamond, the OLC and bulk graphite. From the XRD pattern of the nanodiamond shown in Figure 3(a), it is clear that the diffraction pattern of the nanodiamond showed three broader peaks located at $2\theta = 43.8^\circ$, 75.2° and 91.0°, respectively, corresponding to the (1 1 1), (2 2 0) and (3 1 1) diffraction planes of the nanodiamond, which demonstrated that the nanodiamond crystal was cubic. Another broad peak located at $2\theta = 25.0^\circ$, corresponding to the (0 0 2) diffraction plane of nanographite, could be observed in Figure 3(a). All the diffraction peaks in Figure 3 were obviously broadened due to the very small crystallite size, strains and defects of the nanodiamond and the nanographite [24]. There was a stronger background at the lower angle, ($<15^\circ$) distinct for the whole spectrum, suggesting that there was a certain amount of amorphous carbon still existing in the nanodiamond powder synthesised by detonation.

Figure 3(b) and (c) shows the XRD patterns of the OLC annealed the nanodiamond for 1 h and at the temperature of 1150°C and bulk graphite, respectively. In Figure 3(b), two stronger and broader peaks locating at $2\theta = 24.9^\circ$ and 43.5° could be clearly observed, corresponding to the (0 0 2) and (1 0 0) diffraction planes of graphite, comparing to the graphite XRD pattern shown in Figure 3(c). However, the diffraction peaks corresponding to the nanodiamond disappeared. Based on this result, it could be concluded that the graphitisation of the nanodiamond had been completed after annealing for 1 h and at the temperature of 1150°C in a vacuum of 2 Pa. The appearance of the broad graphitic (0 0 2) peak came from the onion-like nanographite [25]. The intensity of the (0 0 2) and (1 0 0) onion-like nanographite was lower than that of graphite, respectively, as shown in

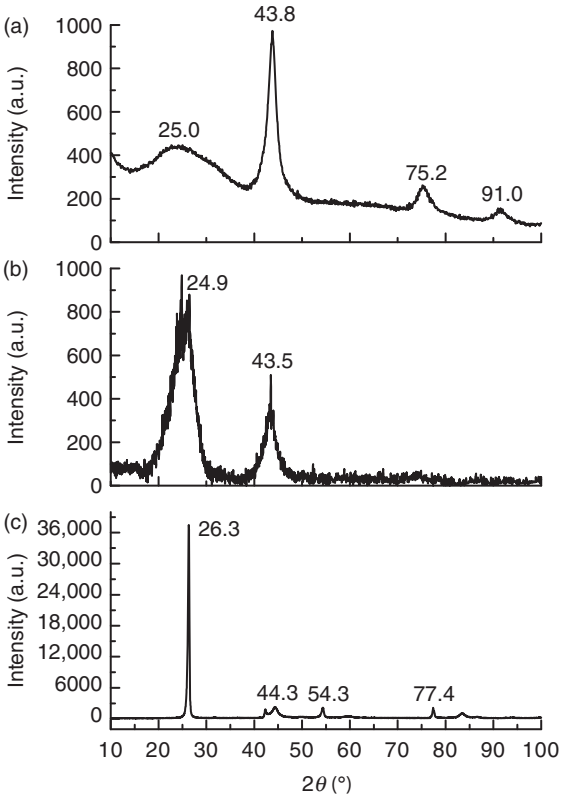

Figure 3. XRD patterns of (a) nanodiamond; (b) OLC; and (c) graphite.

Figure 3(b) and (c), which also demonstrated that the nanodiamond transformed into the OLC under these conditions.

Figure 4 shows the Raman spectra of the nanodiamond, the OLC, the graphite and bulk diamond in the wavenumber range from 400 to 2000 cm^{-1}. From Figure 4(a), we can see that the Raman wide peak in the vicinity of 1335 cm^{-1} is the characteristic peak of the sp^3 structural nanodiamond. Figure 4(d) shows the Raman spectrum for bulk diamond, comparing with the Raman spectrum of the nanodiamond, the peak for the nanodiamond moved to higher frequency, which led from the quantum effects of restrictions [26]. The Raman wide peak in the vicinity of 1603 cm^{-1} is the characteristic peak of the sp^2 structural nanographite existing in the nanodiamond powder. The Raman diffraction peak cross-section of the nanodiamond was approximately 1/70 of the nanographite, which demonstrated that there was still a small quantity of graphite existing in the nanodiamond powder.

Figure 4(b) shows the Raman spectrum of the OLC annealed the nanodiamond for 1 h at the temperature of 1150°C in vacuum of 2 Pa. The graphic (G) mode at approximately 1587 cm^{-1} was usually regarded as a Raman-allowed vibration, corresponding to the optical phonon modes of E_{2g} symmetry in graphite and often called tangential mode for the OLC [27], comparing with the Raman spectrum for bulk graphite

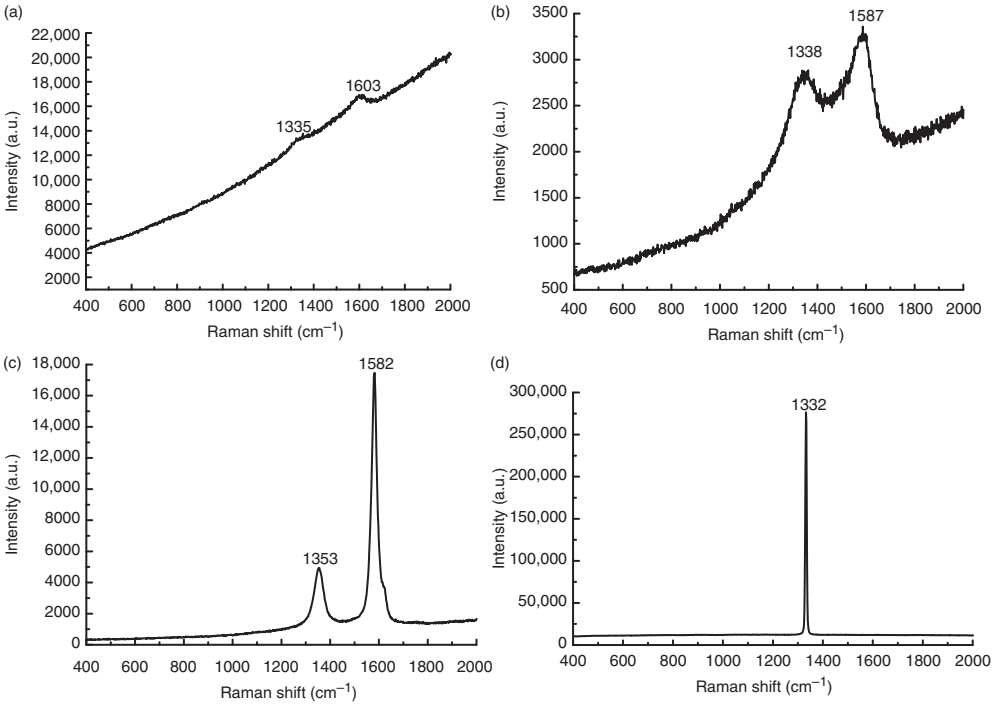

Figure 4. Raman spectra of (a) nanodiamond; (b) OLC; (c) graphite; and (d) bulk diamond.

shown in Figure 4(c). The diamond (D) band at about 1338 cm^{-1} was associated with optical phonons close to the K point of the Brillouin zone in graphite and carbon nanotubes. The weak D-bands demonstrate that the samples contained a very small amount of amorphous carbon, revealing that high-purity OLC was synthesised in this work. This was consistent with the result of the HRTEM image observed, as shown in Figure 1(b). The ratio of the intensities of D–G peak was often used to estimate the degree of perfection of graphene planes [28]. As can be calculated from Figure 4(b), the I_D/I_G ratio was 0.21.

It can be seen from Figure 1(b) that the OLC coexisted with the untransformed nanodiamond existing in the centre of the OLC. These results were in agreement with the XRD results that the OLC coexisted with the nanodiamond when annealed for 1 h at the temperature of 1150°C in a vacuum of 2 Pa, as shown in Figure 3(b). Moreover, it should be noted that there existed diamond (1 1 1) sheets in the centre of the OLC particle and the axis of the OLC was parallel to the original diamond (1 1 1) planes. We believed that the transformation of the OLC from the nanodiamond preferentially began at the (1 1 1) planes of the nanodiamond and the inner nanodiamond had an effect on the outer shells in the shape. It was reasonable that the shape of the OLC particle was similar to that of the original nanodiamond particle. Moreover, the average size of the OLC was approximately 5 nm, which was similar to the size of the nanodiamond particle. Therefore, we proposed that the graphite fragments exfoliating from the nanodiamond (1 1 1) planes enclosed around the surface of the nanodiamond particles gradually and

the OLC particles were developed simultaneously from the nanodiamond particle surface towards the centre.

4. Conclusions

The OLC was fabricated by annealing the nanodiamond synthesised by detonation for 1 h and at the temperature of 1150°C in low vacuum of 2 Pa. The shape and the average size of the OLC were similar to the original nanodiamond particles. The OLC coexisted with the untransformed nanodiamond in the centre. The number of the OLC graphitic shells ranged from several to 12. The interlayer spacing of the OLC was approximately 0.34 nm.

The transformation of the OLC from the nanodiamond preferentially began at the (1 1 1) planes of the nanodiamond and the inner nanodiamond had an effect on the outer shells in the shape. The graphite fragments exfoliating from the nanodiamond (1 1 1) planes enclosed around the surface of the nanodiamond particles gradually and the OLC was developed simultaneously from the nanodiamond particle surface towards the centre.

References

[1] S. Iijima, *Direct observation of the tetrahedral bonding in graphitized carbon black by high resolution electron microscopy*, J. Cryst. Growth 50 (1980), pp. 675–683.
[2] D. Ugarte, *Curling and closure of graphitic networks under electron-beam irradiation*, Nature 359 (1992), pp. 707–708.
[3] T. Oku, T. Hirano, and M. Kuno, *Synthesis, atomic structures and properties of carbon and boron nitride fullerene materials*, Mater. Sci. Eng. B 74 (2000), pp. 206–217.
[4] S. Seraphin, D. Zhou, and J. Jiao, *Filling the carbon nanocages*, J. Appl. Phys. 80 (1996), pp. 2097–2104.
[5] R.K. Rana, Y. Koltypin, and A. Gedanken, *Synthesis of carbon nanotubes from in situ generated cobalt nanoparticles and carbon monoxide*, Chem. Phys. Lett. 344 (2001), pp. 256–262.
[6] N. Sano, H. Wang, and I. Alexandrron, *Properties of carbon onions produced by an arc discharge in water*, J. Appl. Phys. 92 (2002), pp. 2783–2788.
[7] K. Bubke, H. Gnewuch, and M. Henpstead, *Optical anisotropy of dispersed carbon nanotubes induced by an electric field*, Appl. Phys. Lett. 71 (1997), pp. 1906–1908.
[8] A.F. Hebard, M.J. Rosseinsky, and R.C. Haddon, *Superconductivity at 18 K in potassium-doped C_{60}*, Nature 350 (1991), pp. 600–601.
[9] A. Hirate, M. Igarashi, and T. Kaito, *Study on solid lubricant properties of carbon onions produced by heat treatment of diamond clusters or particles*, Tribol. Int. 37, (2004), pp. 899–905.
[10] S.Y. Liu and S.Q. Sun, *Recent progress in the study of endohedral metallofullerenes*, J. Organomet. Chem. 599 (2000), pp. 75–86.
[11] P.J.F. Harris and S.C. Tsang, *Encapsulating uranium in carbon nanoparticles using a new technique*, Carbon 36 (1998), pp. 1859–1861.
[12] S. Barazzouk, S. Hotchandani, and K. Vinodgopal, *Single-wall carbon nanotube films for photocurrent generation. A prompt response to visible-light irradiation*, J. Phys. Chem. B 108 (2004), pp. 17015–17018.
[13] G. Girishkumar, K. Vinodgopal, and P.V. Kamat, *Carbon nanostructures in portable fuel cells: Single-walled carbon nanotube electrodes for methanol oxidation and oxygen reduction*, J. Phys. Chem. B 108 (2004), pp. 19960–19966.
[14] D. Ugarte, *Graphitic nanoparticles*, MRS Bull. 19 (1994), pp. 39–42.

[15] V.L. Kuznetsov, A.L. Chuvilin, Y.V. Butenko, I.Y. Malkov, and V.M. Titov, *Raman and photoluminescence spectra of diamond particles with 1–5 nm diameter*, Chem. Phys. Lett. 222 (1994), pp. 343–348.
[16] X.H. Chen, F.M. Deng, J.X. Wang, H.S. Yang, G.T. Wu, and X.B. Zhang, *New method of carbon onion growth by radio-frequency plasma-enhanced chemical vapor deposition*, Chem. Phys. Lett. 336 (2001), pp. 201–204.
[17] N. Sano, H. Wang, I. Alexandrou, M. Chhowalla, K.B.K. Teo, and K. Iimura, *Properties of nano carbon particles produced by an arc discharge in water*, J. Appl. Phys. 92 (2002), pp. 2783–2790.
[18] Z.J. Qiao, J.J. Li, N.Q. Zhao, C.S. Shi, and P. Nash, *Graphitization and microstructure transformation of nanodiamond to onion-like carbon*, Scr. Mater. 54 (2006), pp. 225–229.
[19] L.G. Bulusheva, A.V. Okotrub, V.L. Kuznetsov, and D.V. Vyalikh, *Soft X-ray spectroscopy and quantum chemistry characterization of defects in onion-like carbon produced by nanodiamond annealing*, Diamond Relat. Mater. 16 (2007), pp. 1222–1226.
[20] N.R. Greiner, D.S.P. Johnson, and F. Volk, *Diamonds in detonation soot*, Nature 333 (1988), pp. 440–442.
[21] Q. Zou, Y.G. Li, L.H. Zou, and M.Z. Wang, *Characterization of structures and surface states of the nanodiamond synthesized by detonation*, Mater. Charact. 60 (2009), pp. 1257–1262.
[22] V.V. Danilenko, *Diamond Synthesis and Sintering by Explosion*, Energoatomizdat, Moscow, 2003.
[23] V.Y. Dolmatov, *Detonation synthesis of ultradispersed diamonds: Properties and applications*, Russ. Chem. Rev. 70 (2001), pp. 607–626.
[24] A.S. Barnard, S.P. Russo, and I.K. Snook, *Structural relaxation and relative stability of nanodiamond morphologies*, Diamond Relat. Mater. 12 (2003), pp. 1867–1872.
[25] J. Qian, C. Pantea, J. Huang, T.W. Zerda, and Y. Zhao, *Graphitization of diamond crystals of different sizes at high pressure-high temperature*, Carbon 42 (2004), pp. 2691–2697.
[26] J. Chen, S.Z. Deng, J. Chen, Z.X. Yu, and N.S. Xu, *Graphitization of nanodiamond powder annealed in argon ambient*, Appl. Phys. Lett. 24 (1974), pp. 3651–3653.
[27] H. Zeng, L. Zhu, G.M. Hao, and R.S. Sheng, *Synthesis of various forms of carbon nanotubes by AC arc discharge*, Carbon 36 (1998), pp. 259–261.
[28] F. Tuinstra and J.L. Koenig, *Raman spectrum of graphite*, J. Chem. Phys. 53 (1970), pp. 1126–1131.